Available online at www.sciencedirect.com
SCIENCE DIRECT®
Geoderma 134 (2006) 373–385
GEODERMA
www.elsevier.com/locate/geoderma

Multifractal characterization of saprolite particle-size distributions after topsoil removal

J.G.V. Miranda [a], E. Montero [b], M.C. Alves [c], A. Paz González [d,*], E. Vidal Vázquez [e]

[a] *Instituto de Física, Universidade Federal da Bahia, Brazil*
[b] *Dept. de Matemática y Física Aplicada, Universidad Alfonso X el Sabio, Spain*
[c] *Faculdade de Engenharia de Ilha Solteira, Universidade Estadual Paulista, Brazil*
[d] *Facultad de Ciencias, Universidade da Coruña, Spain*
[e] *Escuela Politécnica Superior, Universidade de Santiago de Compostela, Spain*

Available online 19 April 2006

Abstract

Multifractal analysis is now increasingly used to characterize soil properties as it may provide more information than a single fractal model. During the building of a large reservoir on the Parana River (Brazil), a highly weathered soil profile was excavated to a depth between 5 and 8 m. Excavation resulted in an abandoned area with saprolite materials and, in this area, an experimental field was established to assess the effectiveness of different soil rehabilitation treatments. The experimental design consisted of randomized blocks. The aim of this work was to characterize particle-size distributions of the saprolite material and use the information obtained to assess between-block variability. Particle-size distributions of the experimental plots were characterized by multifractal techniques. Ninety-six soil samples were analyzed routinely for particle-size distribution by laser diffractometry in a range of scales, varying from 0.390 to 2000 μm. Six different textural classes (USDA) were identified with a clay content ranging from 16.9% to 58.4%. Multifractal models described reasonably well the scaling properties of particle-size distributions of the saprolite material. This material exhibits a high entropy dimension, D_1. Parameters derived from the left side ($q>0$) of the $f(\alpha)$ spectra, D_1, the correlation dimension (D_2) and the range ($\alpha_0-\alpha_{q+}$), as well as the total width of the spectra ($\alpha_{max}-\alpha_{min}$), all showed dependence on the clay content. Sand, silt and clay contents were significantly different among treatments as a consequence of soil intrinsic variability. The D_1 and the Holder exponent of order zero, α_0, were not significantly different between treatments; in contrast, D_2 and several fractal attributes describing the width of the $f(\alpha)$ spectra were significantly different between treatments. The only parameter showing significant differences between sampling depths was ($\alpha_0-\alpha_{q+}$). Scale independent fractal attributes may be useful for characterizing intrinsic particle-size distribution variability.

Keywords: Multifractal analysis; Soil restoration; Particle-size distribution; Oxisol; Saprolite

1. Introduction

Natural soils are the result of pedogenetic processes that are governed by soil-forming factors, namely parent material, climate, relief, biosphere, water and time. Land use by man can have an effect on all the above soil-forming factors and, in some cases, can severely change or even destroy natural soil profiles.

* Corresponding author. Tel. : +34 981 167000; fax: +34 981 167065.
E-mail addresses: vivas@ufba.br (J.G.V. Miranda), elomont@terra.es (E. Montero), mcalves@agr.feis.unesp.br (M.C. Alves), tucho@udc.es (A. Paz González), evavidal@lugo.usc.es (E. Vidal Vázquez).

0016-7061/$ - see front matter © 2006 Elsevier B.V. All rights reserved.
doi:10.1016/j.geoderma.2006.03.014

Soil is now viewed as a multifunctional medium. It is a substrate for agricultural production; it forms an essential part of the landscape, provides raw materials and conserves the remains of our past. However, soil is a limited and non-renewable resource so damage to soil is not easily repaired.

Soil use, as a structural and foundation material for engineering purposes, is widespread and results in artificially disturbed landscapes. Unless reclamation measures are undertaken (such as soil replacement, landscaping or establishment of vegetation cover), at many construction sites, soil disturbances may continue for years. Construction of reservoirs and associated facilities in São Paulo State (Brazil), such as roads, buildings and earthworks, was achieved by engineering practices which included the manipulation and disturbance of deep soil profiles with highly weathered soil horizons. Natural soil profiles were excavated and 5–8 m of topsoil removed, exposing an underlying saprolitic material (Alves, 2001). This profile decapitation caused a drastic reduction in soil biota, which resulted in loss of stability of both the above ground plant community and the soil community itself with loss of ecosystem function. As a consequence, this soil, with a long natural history and influenced by agricultural activities, was not only degraded but also consumed so that it was no longer productive.

Disturbed areas left after surface and subsurface soil removal are not necessarily lost to agriculture or alternative land uses. Current interest in improving soil quality (an issue which is also linked to sustainable development) should not only focus on agricultural and natural soils but also on degraded soils and raw materials exposed at the earth surface (EEA, 2000). Land use and soil management systems are sustainable only if they maintain or improve soil quality and do not compromise environmental quality (Doran and Parkin, 1994; Carter et al., 1997; Gregorich, 2002). Improved soil quality increases the ability of a soil to fulfil its functions, including crop productivity, water and nutrient storage, and filtering and buffering of pollutants, thereby reducing contamination of surface and groundwater bodies by erosion or leaching processes.

During the building of a large reservoir on the Parana River, a highly weathered soil profile was excavated at Selvíria, Brazil. The saprolitic material exposed at the site was less resilient and that motivated this study. There was no pioneer vegetation growth after the abandonment and also further degradation by erosion was apparent. This motivated the installation of field trials to test the efficiency of different revegetation strategies.

The experimental design consisted of randomized blocks. In field trials, it is currently assumed without further testing that basic soil properties and parameters influencing fertility status and plant production are randomly distributed; hence, they do not significantly differ between plots with different treatments. This assumption has been strongly criticized, since, on the one hand, structured horizontal spatial variability has been often reported using geostatistical techniques (Vieira et al., 1983; Solie et al., 1999; Paz González et al., 2000) and, on the other hand, local or global trends may produce a bias in soil attributes involving blocks of a specific treatment. Structured variation in soil spatial properties between and within blocks may obscure the results of field trials.

Soil texture is one of the main properties characterizing a soil. The particle-size distribution of a given horizon is the result of the interaction between soil-forming processes and factors. Proper characterization of particle-size distribution is needed to quantify the various processes it influences. Soil mechanical composition is commonly expressed as percentage of clay, silt and sand contents and represented in a textural triangle, but a textural class contains limited information for assessing particle-size distributions (Martín and Taguas, 1998; Martín and Rey, 2000; Martín et al., 2001; Posadas et al., 2001). In spite of this, a number of different approaches have been developed to model and characterize particle-size distributions (see Montero, 2005 for a review). It has been stated that the main objective in characterizing soil particle-size distributions should be to find quantities or parameters that capture the essence of the phenomena and also that new concepts are required for this purpose (Martín and Taguas, 1998; Martín and Rey, 2000; Martín et al., 2005).

Over the last few decades, much attention has been paid to quantitative studies of soil texture and other physical parameters using the concept of fractal geometry. Fractal models were recognized as valuable tools in the description, quantification and modeling of soil properties varying as a function of observation scale. Scaling effects have been frequently observed in soil properties and attributes, so they are thought to be more the rule than the exception. Within this framework, a measure no longer appears to be a single number or a mean value with a confidence interval, but rather a function of the scale. In the simplest case, when self-similarity at every measurement scale is evidenced, the function of scale is a power law and the exponent of the power law depends only on the so-called fractal dimension, D. This single scaling exponent has been

used in the past to characterize a fractal object (Turcotte, 1986; Tyler and Wheatcraft, 1992).

Models based on a single fractal dimension do not adequately describe soil particle and pore size distributions (Kravchenko et al., 1999; Caniego et al., 2001; Martín et al., 2001; Posadas et al., 2001, 2003; Montero, 2005). Moreover, mass and pore distributions in a range of scales, such as those occurring in soils, are characterized by fractal dimensions that vary in scale and so require an infinite number of scaling exponents for their description. This type of fractal behavior is termed multifractal. The reason for the observed heterogeneity is thought to be due to variations in particle or pore density across different length scales. A multifractal analysis captures the inner variations in a system by resolving local densities and expressing them by a distributional spectrum (Feder, 1988; Kravchenko et al., 1999; Caniego et al., 2001). This approach is well suited to soil analysis because soil properties are determined by several soil-forming factors and processes operating at different scales.

Single and multifractal techniques have been applied to the study of particle-size distributions in soils. The results obtained using models based on a single fractal dimension have been summarized and the limitations of such an approach stressed (Posadas et al., 2001; Montero, 2005). Multifractal techniques were first used by Grout et al. (1998) to characterize particle-size distributions of heavy textured soils. Posadas et al. (2001) applied multifractal analysis to soil samples covering a wide range of textural classes. More recently, different data sets of particle-size distributions have been characterized by their multifractal spectra (Martín and Montero, 2002; Montero and Martín, 2003; Martín et al., 2005). Parameters obtained from fractal analysis could also be useful for a description of spatial variability.

Particle-size distributions from the residual saprolite material sampled at the experimental plots of the above-mentioned field trial were measured by laser diffractometry. The first objective of this work was to characterize, by means of multifractal techniques, particle-size distributions of the new developing soil profile in the experimental plots. In addition, the question of the usefulness of the information obtained from the multifractal particle-size distribution spectrum for assessing between treatment variability and for optimizing design strategies was addressed.

2. Background

In this section, fractal theory and concepts are briefly summarized with particular emphasis on multifractal techniques. Formal mathematical derivations have been omitted. More detailed information can be found in Voss (1988), Meakin (1991), and Vicsek (1992). Other summaries of multifractal estimation methods include Grout et al. (1998), Kravchenko et al. (1999), Caniego et al. (2001), Posadas et al. (2001, 2003), Montero (2005), etc. Most of these publications have been somewhat selective, or have focused on a specific attribute within soil science.

As an introduction to multifractals, let us consider an irregular mass or pore pattern or some other feature that contains an internal structure repeated over a range of scales. This distribution will represent a monofractal if the number of features N of a certain size ε varies following a power scaling law as:

$$N(\varepsilon) \sim \varepsilon^{-D} \tag{1}$$

where D is the fractal dimension. The relation defined in Eq. (1) is a scaling law that has been frequently used to describe the size distribution of many natural objects.

Multifractal methods can also resolve much more heterogeneous patterns in regions that have locally high or low accumulations of mass. If we consider again a complex spatial arrangement of mass and a grid of boxes of length ε is laid over this pattern, box densities can be expressed as a proportion by estimating the mass probability, p_i, in an ith box, according to:

$$p_i(\varepsilon) = \frac{N_i(\varepsilon)}{N_t} \tag{2}$$

where $N_i(\varepsilon)$ is the mass of the ith box and N_t is the total mass of the system.

Thus, for a multifractal measure, this probability will scale with different exponents for each box of size ε unit as:

$$p_i(\varepsilon) \sim \varepsilon^{-\alpha_i} \tag{3}$$

where α_i is the coarse Holder, or singularity, exponent for boxes, which theoretically represents how singularities of the systems tend to infinity in the limit as $\varepsilon \to 0$.

To obtain the multifractal spectrum of this distribution an evaluation of the number of boxes that have a specific α exponent N_α is required. In a way similar to Eq. (1), in the case of multifractal patterns, this measure will scale as:

$$N_\alpha(\varepsilon) \sim \varepsilon^{-f(\alpha)} \tag{4}$$

where the set of $f(\alpha)$ values represents the spectrum of fractal dimensions that characterize the abundance of the set of points with singularity α.

Multifractal measures can also be characterized by means of the scaling of the qth moments of $\{p_i\}$ distributions (Chhabra and Jensen, 1989), which is expressed in the form:

$$\mu(q,\varepsilon) = \sum_{i=1}^{N(\varepsilon)} p_i^q(\varepsilon) \quad (5)$$

In Eq. (5), for $q>0$, regions in the distribution having a high degree of a measure are magnified, whereas the opposite is true for $q<0$.

The generalized fractal dimensions or Rényi dimensions can be computed by:

$$D_q = \frac{1}{q-1}\lim_{\varepsilon\to 0}\frac{\log\mu(q,\varepsilon)}{\log\varepsilon} \quad (6)$$

Note that, for a monofractal, D_q is a constant function of q, so no additional information is obtained by examining higher moments. For multifractal measures, the relationship between D_q and q is not constant. In this case, the most frequently used generalized dimensions are those for $q=0$, $q=1$ and $q=2$ termed, respectively, D_0 or capacity dimension, D_1 or entropy (Shannon) dimension, and D_2 or correlation dimension. The capacity or box-counting dimension, D_0, is independent of the quantity of mass in each box; it is the scaling exponent of the number of non-empty boxes.

3. Materials and methods

3.1. Experimental site

The study area is located in Selviría (MS-Brazil) 51°22″W and 20°22″S. The undisturbed soil, developed over clay sediment, was classified as Oxisol, according to the Soil Survey Staff (1993), Ferralsol (FAO, 1998) or Latossolo in the Brazilian Soil Classification System (EMBRAPA, 1999). Beginning in 1960, a 5–8-m deep layer of this soil was removed for earthworks during construction of a large reservoir on the Parana River. Excavation resulted in an abandoned area with saprolite materials and in this area an experimental field was established. A revegetation experiment started in 1992, where field trials were established to evaluate different amendment and fertilization treatments on the former subsoil, now exposed at the surface (Fig. 1a). The experimental randomized design consisted of seven different treatments inside the revegetated area and one additional treatment on the raw material outside this area (Fig. 1b). Each of the eight treatments was replicated four times using plots measuring 10 m long by 10 m wide, so that a total of 32 plots were studied.

The management systems of the study area consisted of eight treatments, one external control on never-tilled non-cultivated raw saprolite and seven tilled treatments with different amendments and green manure addition strategies on the revegetated experimental area. The seven cultivated treatments were first tilled in 1992, and between 1992 and 1997 they received different lime amendments and green manure applications. The eight treatments were as follows:

0. External control: residual saprolite without any tillage treatment.
1. Control treatment within the tilled area, without culture and without any green manure.
2. Culture of mucuna (*Stizolobium aterrimun* Piper and Tracy) used as green manure.
3. Culture of canavalia (*Canavalia ensiformis* (L.) DC) used as green manure.
4. Lime addition and culture of mucuna used as green manure.
5. Lime addition and culture of canavalia used as green manure.
6. Lime plus gypsum addition and culture of mucuna used as green manure.
7. Lime plus gypsum addition and culture of canavalia used as green manure.

On all the plots of the experimental area (treatments 1 to 7), maize (*Zea mays* L.) was sown in 1997 and later on oats variety (*Avena strigosa* Schieb) and brachiaria (*Brachiaria decumbens* Stapf) were sown in 1998 and 1999, respectively.

Soil samples were collected in 2001, 9 years after reestablishment of vegetation on the saprolite horizon. Sampling was performed at three depths (0–10 cm, 10–20 cm and 20–40 cm) in each plot, giving a total of 96 individual samples. Soil samples were dried and sieved through a 2-mm sieve.

3.2. Particle-size distribution analysis

Soil samples were analyzed routinely for particle-size distribution. The procedure has two steps: dispersion and fractionation. As dispersion agents, first hydrogen peroxide (H_2O_2) to remove organic material and second sodium dithionite to remove sesquioxides were used. After dispersion, soil samples were fractionated by laser diffractometry in a range of scales varying from 0.390 to 2000 μm, using a Coulter LS 120 instrument. The

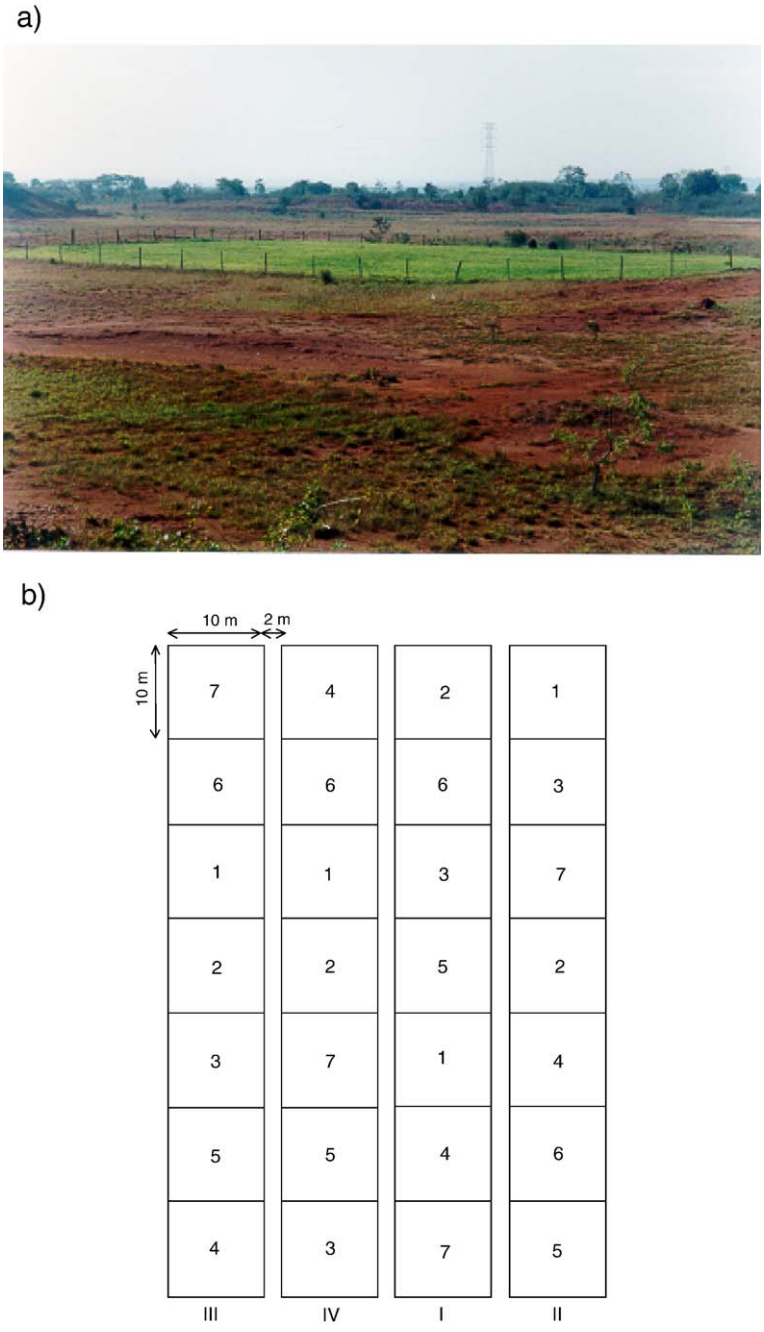

Fig. 1. (a) Photo of the experimental area when soil was sampled. (b) Scheme showing the experimental revegetated area with treatments 1 to 7. Treatment 0 was raw material outside this area.

number of measured intervals was 83 for each particle-size distribution (Paz Ferreiro, 2002).

The soil textures were far from homogeneous, showing sand contents in the range 1.6–39.6%, silt contents of 32.8–57.1% and clay contents of 16.9–51.8%. The distribution of sand, clay and silt in the textural triangle for the 96 samples of the study data set is shown in Fig. 2. Six textural classes can be distinguished within this database, of which four are medium textured (clay loam, loam, silt loam, silty clay loam) and two heavy textured (silty clay and clay). The highest variability in clay contents was observed at the

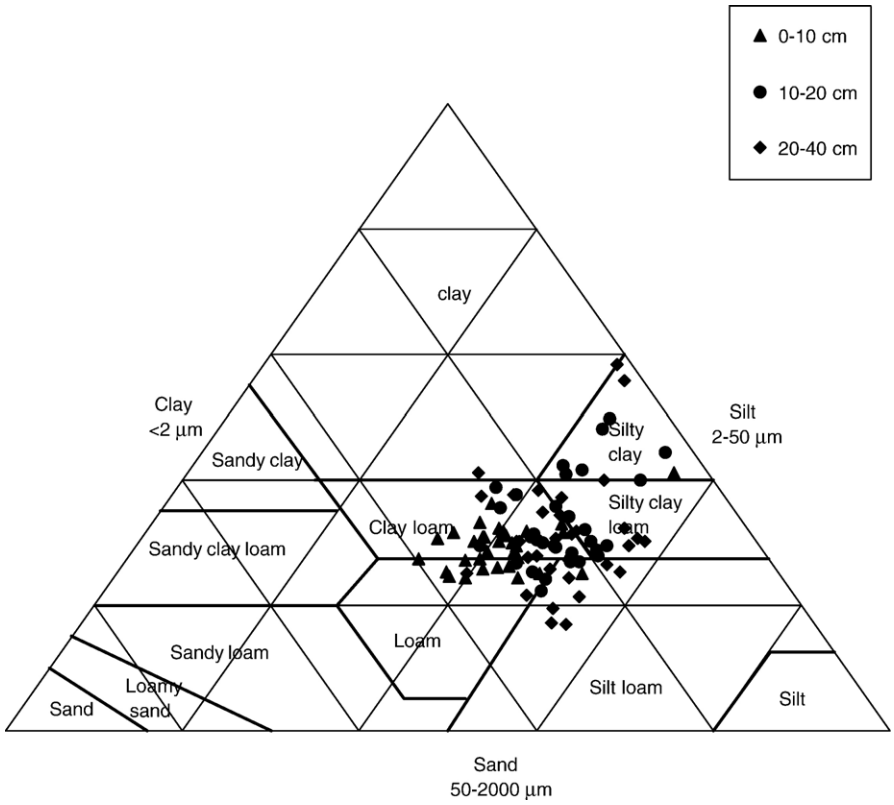

Fig. 2. Soil textural triangle showing the range of textures studied as a function of depth (Soil Survey Staff, 1993).

10–20-cm sampling depth, whereas samples at the 0–10-cm depth exhibited more homogeneous clay content.

3.3. Determination of multifractal parameters

To obtain the multifractal spectra $f(\alpha)$, the method proposed by Chhabra and Jensen (1989) was applied, because of its simplicity and precision when applied to experimental data. This method establishes a parametric way to estimate separately $f(\alpha(q))$and $\alpha(q)$ values:

$$\sum_{i=1}^{N(\varepsilon)} \mu_i(q,\varepsilon)\log[p_i(\varepsilon)] \sim \alpha(q)\log(\varepsilon) \quad (7)$$

$$\sum_{i=1}^{N(\varepsilon)} \mu_i(q,\varepsilon)\log[\mu_i(q,\varepsilon)] \sim f[\alpha(q)]\log(\varepsilon) \quad (8)$$

where $\mu_i(q,\varepsilon)$ is the normalized measure and is defined as:

$$\mu_i(q,\varepsilon) = \frac{p_i^q(\varepsilon)}{\sum_{i=1}^{N(\varepsilon)} p_i^q(\varepsilon)} \quad (9)$$

The α and $f(\alpha)$ values are obtained by linear regression applied to Eqs. (7) and (8), respectively. The α and $f(\alpha)$ parameters are not evaluated for all values of q, but rather in the range in which they can be described by a straight line function of log ε, representing the level of heterogeneity of the sample. So, for regressions with $R^2 > 0.90$, the point $(\alpha, f(\alpha))$ is accepted in the experimental spectrum.

The analysis of the particle-size distribution measures was performed as proposed by Martín and

Table 1
Mean sand, silt and clay contents of the study treatments

Treatment	Sand	Silt	Clay
0	25.79 a	44.32 bcd	29.89 bcd
1	26.68 a	43.39 cde	29.93 bcd
2	20.68 b	48.38 a	30.94 bc
3	26.22 a	40.16 e	33.62 ab
4	23.45 ab	40.10 de	34.46 ab
5	13.90 c	48.59 a	37.51 a
6	25.92 a	46.55 abc	27.54 cd
7	27.04 a	47.26 ab	25.70 d

Values followed by the same letter do not differ statistically (Duncan test at the 95% confidence level).

Montero (2002) and Montero (2005). The measure $\mu_i(\varepsilon)$ over the distribution was computed from the relative volume data, v_i; first V_i are normalized, $V_i=(v_i/\sum_i v_i)$, $i=1,2,..,92$, with $\sum_{i=1}^{92} V_i=1$, and then the measure $\mu_i(\varepsilon)$ assigned to those blocks was computed by adding all contributions V_i inside a box. The interval calculated for the scales is logarithmically spaced. The range of scales in the available data varied from 0.393 to 1909 μm. The range of scales used to fit Eqs. (7) and (8) was [1.66, 43.7] μm, which in logarithmic scale represents 1/16 and 1/2, respectively, of the total range.

3.4. Statistical analysis

Statistical analyses, i.e. linear regression analysis and analysis of variance (ANOVA), were performed using the SAS package, version 8.0 (SAS Institute, 1999). A total of 96 experimental data sets (i.e. 8 treatments × 4 replications × 4 depths) were parameterized. Treatment differences were evaluated by comparison of means using the Duncan test.

4. Results and discussion

4.1. Statistical analysis of texture

Taking into account the mean sand, silt and clay contents for all the management systems, statistically significant differences were observed for some treatments, as shown in Table 1. The lowest mean sand content (13.90%) was found in the random plots of treatment 5 and this value was statistically different from those of the other seven treatments at the 95% confidence level. The mean sand content of treatment 2 (20.68%) was also significantly different at the 95% confidence level from

Table 2
Main parameters from multifractal analysis of particle-size distributions

Sample	T and R[a]	q_-	q_+	D_1	r^2	D_2	r^2	α_0	r^2	α_{min}	α_{max}
1	0-I	−0.8	10	0.954±0.007	0.9997	0.900±0.010	0.9990	1.090±0.010	0.9994	0.804	1.616
2	1-I	−1.2	8.4	0.966±0.005	0.9999	0.935±0.002	1.0000	1.056±0.007	0.9998	0.853	1.522
3	2-I	−1	8.6	0.966±0.003	0.9999	0.870±0.003	0.9999	1.064±0.006	0.9999	0.891	1.561
4	3-I	−3.8	7.6	0.981±0.001	1.0000	0.933±0.008	0.9997	1.020±0.002	1.0000	0.850	1.207
5	4-I	−3.8	4.6	0.966±0.002	1.0000	0.941±0.009	0.9996	1.035±0.003	1.0000	0.816	1.270
6	5-I	−2	10	0.981±0.003	1.0000	0.961±0.002	1.0000	1.027±0.004	0.9999	0.923	1.355
7	6-I	−1	9	0.957±0.003	0.9999	0.890±0.010	0.9990	1.074±0.006	0.9999	0.804	1.661
8	7-I	−2	6.2	0.975±0.005	0.9999	0.947±0.002	1.0000	1.030±0.007	0.9998	0.869	1.297
9	0-II	−4.8	6.4	0.983±0.002	1.0000	0.945±0.001	1.0000	1.017±0.002	1.0000	0.856	1.160
10	1-II	−1.6	7.4	0.971±0.002	1.0000	0.959±0.006	0.9998	1.041±0.004	0.9999	0.851	1.465
11	2-II	−2.2	10	0.987±0.002	1.0000	0.942±0.001	1.0000	1.018±0.004	0.9999	0.951	1.237
12	3-II	−0.8	10	0.948±0.007	0.9998	0.921±0.007	0.9997	1.100±0.010	0.9994	0.754	1.816
13	4-II	−1.4	6.2	0.972±0.004	0.9999	0.931±0.008	0.9997	1.038±0.008	0.9997	0.864	1.334
14	5-II	−1.6	10	0.972±0.004	0.9999	0.929±0.004	0.9999	1.042±0.006	0.9998	0.906	1.428
15	6-II	−0.8	4.4	0.928±0.009	0.9996	0.910±0.010	0.9994	1.110±0.010	0.9996	0.737	1.828
16	7-II	−2	4.8	0.972±0.002	1.0000	0.933±0.007	0.9997	1.033±0.005	0.9999	0.835	1.300
17	0-III	−10	4.4	0.968±0.001	1.0000	0.969±0.006	0.9999	1.030±0.001	1.0000	0.795	1.218
18	1-III	−1	7.8	0.964±0.002	1.0000	0.947±0.003	0.9999	1.060±0.008	0.9997	0.801	1.509
19	2-III	−2.2	7.4	0.981±0.003	0.9999	0.796±0.040	0.9917	1.022±0.005	0.9999	0.871	1.220
20	3-III	−1.6	7.6	0.966±0.003	0.9999	0.948±0.005	0.9999	1.043±0.006	0.9999	0.794	1.373
21	4-III	−2.8	3.6	0.961±0.001	1.0000	0.947±0.007	0.9998	1.039±0.003	1.0000	0.784	1.266
22	5-III	−1.6	7.6	0.970±0.003	1.0000	0.920±0.020	0.9987	1.046±0.003	1.0000	0.852	1.528
23	6-III	−2	5.8	0.957±0.005	0.9999	0.880±0.020	0.9987	1.050±0.004	0.9999	0.779	1.406
24	7-III	−2.8	4.6	0.969±0.002	1.0000	0.940±0.010	0.9994	1.032±0.003	1.0000	0.818	1.265
25	0-IV	−1.2	8.6	0.970±0.004	0.9999	0.943±0.006	0.9998	1.049±0.007	0.9998	0.855	1.489
26	1-IV	−1	8.2	0.966±0.005	0.9999	0.966±0.005	0.9999	1.060±0.009	0.9997	0.856	1.525
27	2-IV	−1	9.6	0.962±0.007	0.9998	0.940±0.003	0.9999	1.070±0.010	0.9996	0.861	1.560
28	3-IV	−2.2	4.4	0.967±0.004	0.9999	0.930±0.010	0.9992	1.036±0.006	0.9998	0.820	1.299
29	4-IV	−3	5.2	0.975±0.002	1.0000	0.964±0.006	0.9998	1.027±0.003	1.0000	0.846	1.233
30	5-IV	−1.6	4.8	0.974±0.004	0.9999	0.967±0.008	0.9997	1.034±0.006	0.9999	0.827	1.337
31	6-IV	−1.6	10	0.974±0.003	1.0000	0.948±0.005	0.9999	1.035±0.004	0.9999	0.824	1.370
32	7-IV	−2.8	9.2	0.983±0.002	1.0000	0.964±0.007	0.9998	1.020±0.002	1.0000	0.872	1.251

Depth, 0–10 cm.
[a] T = treatment and R = repetition.

all the other treatments except treatment 4. Silt content was lowest in treatment 3 (40.16%) and highest in treatment 5 (48.59%); mean values of silt content in treatments 1, 3 and 4 were significantly different at the 95% confidence level from those of treatments 2, 5, 6 and 7. One important result, also observed through the Duncan test, lies in that the mean clay contents of treatments 3, 4 and 5 were statistically different from those of treatments 0, 1, 6 and 7.

The Duncan average comparison test also showed that there were statistically significant differences between the three sampled layers at the 95% confidence level (data not shown). The mean sand content at the 0–10-cm layer was significantly higher than at the 10–20-cm and 20–40-cm layers. Opposite to this, the mean silt content of the 0–10-cm layer was lowest and significantly different at the 95% confidence level from that of the other two layers. Also, the mean clay content at the 0–10-cm depth was significantly different from that at the 10–20-cm depth. There was no interaction between treatment and depth according to the above-mentioned test.

The presence of statistical differences among treatments and depths indicates that the texture was far from homogeneous in space over the study area. In other words, at the sampling scale a substantial spatial variability of the sand, silt and clay amounts of the different treatments was observed, and these soil properties were not randomly distributed.

4.2. Multifractal analysis

Selected parameters obtained by multifractal analysis for the 0–10-cm depth are listed in Table 2. For a multifractal system, the moments of order q over which fractal behavior is applicable cover a limited range of scales. This is because the first and one of the most important steps in multifractal analysis is to determine the range of ε and q exhibiting linear behavior when fitting Eqs. (7) and (8). The range of q values in our work was selected by taking into account coefficients of determination, R^2, of the fitted straight-line equal to or greater than 0.90. Thus, $f(\alpha)$ spectra were computed in the range $-10<q<10$ for successive 0.2 steps, and the upper and lower limits of

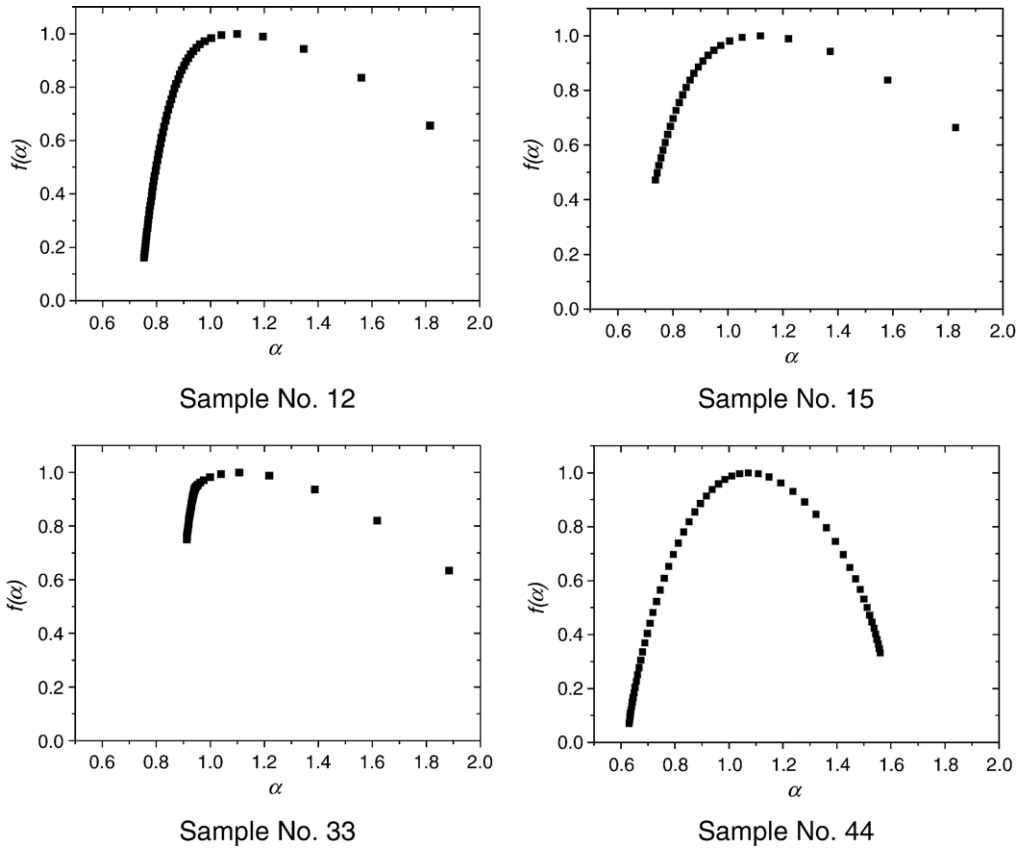

Fig. 3. Selected examples of $f(\alpha)$ spectra.

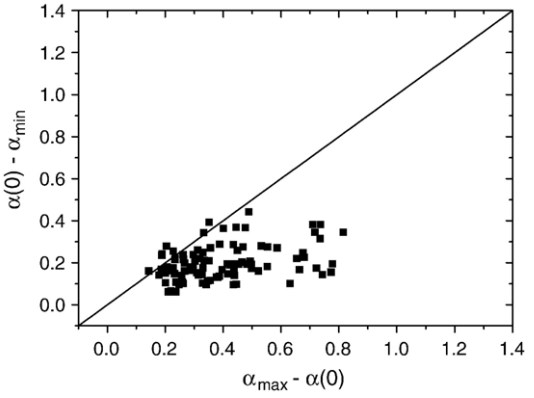

Fig. 4. Relationship between the ranges of the left ($\alpha_0-\alpha_{min}$) and right ($\alpha_{max}-\alpha_0$) sides of the $f(\alpha)$ spectra.

multifractal behavior were selected with the aid of the 0.90 threshold of the determination coefficients.

The largest variation in Δq was observed in the range of positive q values. Minimum Δq_+ was 2.8 and 31 out of 96 particle-size distributions reached the maximum $\Delta q_+=10.0$. In contrast, Δq_- ranged from −0.8 to −10.0, but only 2 out of 96 samples reached the lower limit $\Delta q_-=-10.0$, while 73 out of 96 showed Δq_- less than or equal to 2.0.

The $f(\alpha)$ spectra showed a range of curvature types and symmetry. The shape and symmetry of the $f(\alpha)$ spectra allowed the assessment of the heterogeneity of the particle-size distributions. The variety of $f(\alpha)$ spectra found in this study is illustrated by selected examples shown in Fig. 3. All plots are characterized by a typical concave parabolic shape, but exhibit very different symmetry features.

Three of the selected $f(\alpha)$ spectra in Fig. 3 (samples 12, 15 and 33) were strongly asymmetric, so the range of their left side ($q>0$) was much smaller than the range of the right side ($q<0$). The texture of samples 12 and 15 was clay loam. Sample number 33, with a loam texture, exhibited the biggest differences between left and right sides of its $f(\alpha)$ spectrum, with apertures $(\alpha_0-\alpha_{q+})=0.195$ and $(\alpha_{q-}-\alpha_0)=0.778$ on the left and right hand sides, respectively. However, the spectrum of sample number 44 was remarkably symmetrical and the ranges $(\alpha_0-\alpha_{q+})=0.442$ and $(\alpha_{q-}-\alpha_0)=0.449$ were reasonably close. The texture of sample 44 was silty clay and the sand content as low as 8.5%.

The width of the $f(\alpha)$ spectrum is defined as the difference between the most positive and negative moments used in the evaluation of the singular spectra and the moment of order zero, i.e. $(\alpha_0-\alpha_{q+})$ and $(\alpha_{q-}-\alpha_0)$. This width may be considered as an indicator of symmetry/asymmetry of a multifractal system.

Values of the determination coefficients of the straight line fitted to the plot of the numerator term in Eq. (7) versus the log of the scale, ε, were highest for $q=0$ (data not shown) and decreased for $q=1$, $q=2$ and successive higher moments of order q. As observed in Table 2, for $q=1$, all 32 samples taken at the 0–10-cm depth were above 0.999 and, for $q=2$, they were above 0.980. The same results were observed for samples at the 10–20- and 20–40-cm depths (data not shown). For all 96 particle-size distributions, the fits used for the evaluation of the singularity spectrum are accurate in the central region, i.e. $-2<q<2$. Thus, in all the cases studied, reliable information was available to test the multifractal behavior of the experimental measures, including parameters D_0, D_1, D_2 and the $f(\alpha)$ spectra.

Values of D_0 were not significantly different from 1. The range of values obtained for D_1 varied between 0.913 and 0.989 and those for D_2 between 0.731 and 0.975. In general, the differences $f(\alpha_0)-f(\alpha_q)$ notably increase as the absolute value of q grows. These results support the hypothesis of singular behavior of the particle-size distributions, since a single fractal would be characterized by the equality of D_0, D_1 and D_2 values.

Heterogeneity of multifractal spectra can be assessed in different ways. For example, the curvature and symmetry of the $f(\alpha)$ spectra provide information on the heterogeneity. In a homogeneous monofractal system

Table 3
Mean values of multifractal parameters of the study treatments

Treatment	α_0	D_1	D_2	$\alpha_{q-}-\alpha_0$	$\alpha_0-\alpha_{q+}$	$\alpha_{max}-\alpha_{min}$
0	1.055 a	0.9658 a	0.9290 a	0.523 ab	0.225 abc	0.749 ab
1	1.046 a	0.9646 a	0.9205 ab	0.406 abc	0.215 bc	0.622 abc
2	1.025 a	0.9797 a	0.9420 a	0.280 c	0.128 c	0.409 c
3	1.043 a	0.9582 a	0.8723 c	0.281 c	0.327 a	0.608 abc
4	1.027 a	0.9703 a	0.8830 bc	0.154 c	0.304 ab	0.458 bc
5	1.033 a	0.9708 a	0.9096 abc	0.336 abc	0.194 bc	0.530 abc
6	1.046 a	0.9643 a	0.9198 ab	0.529 ab	0.207 bc	0.737 ab
7	1.048 a	0.9632 a	0.9191 ab	0.551 a	0.237 abc	0.789 a

Values followed by the same letter do not differ statistically (Duncan test at the 95% confidence level).

the $f(\alpha)$ spectra would be reduced to a single point. A homogeneous multifractal is characterized by a narrow range of $f(\alpha)$ spectra. Heterogeneity can also be assessed by the magnitude of changes around D_0 in both $f(\alpha)$ and α axes (Posadas et al., 2001).

The differences in width of the left and right sides of the $f(\alpha)$ spectra analyzed are shown in Fig. 4. Except for 6 out of 96 samples, the right side of the $f(\alpha)$ spectra exhibits a higher width or aperture than those of the left side. In this type of representation, proximity to line 1:1 is a test of symmetric spectrum. These results indicate that there was a wide range of variability in the heterogeneity of the saprolite samples studied.

Holder exponents of order zero, $\alpha(0)$, and order q, $\alpha(q)$, are parameters that can also be used to distinguish between soil particle-size distributions. Both $\alpha(0)$ and the difference $\alpha(q)-\alpha(0)$ have been used to assess heterogeneity. The value of $\alpha(0)$ quantifies the average scale of mass density (or probability) with scale; in other words, $\alpha(0)$ is the average of the singularity strength of the particle-size distribution. Table 2 shows that the determination coefficients in estimating $\alpha(0)$ were higher than 0.998 for samples taken at 0–10-cm depth. Similar results were obtained for samples taken at 10–20- and 20–40-cm depths (data not shown). The range of $\alpha(0)$ values was rather narrow, between 1.014 and 1.132. The variance analysis showed that this parameter does not allow discrimination between different treatments or samples with different texture (Table 3). The sample with the maximum $\alpha(0)$ exhibited on average the lowest degree of mass concentration, and the opposite was also true, such that the sample with minimum $\alpha(0)$ presented on average the highest degree of local density.

The dimension, D_1, in multifractal systems is directly associated to the entropy of the system and is also an index of the dispersion of the measure. A D_1 value close to D_0 (i.e. maximum entropy) should be an indication of a measure distributed over all the study scales, whereas a D_1 close to 0 should reflect clustering, indicating that most of the measure concentrates in a small size domain of the study scale. As mentioned before, D_1 values calculated in this work for samples taken in the newly developed soil profile showed a very narrow range, only 0.913 to 0.989. Moreover, as illustrated in Fig. 5, most of the particle-size distributions were characterized by D_1 values greater than 0.95. The ANOVA variance analysis also showed that D_1 does not allow discrimination between different management treatments (Table 3).

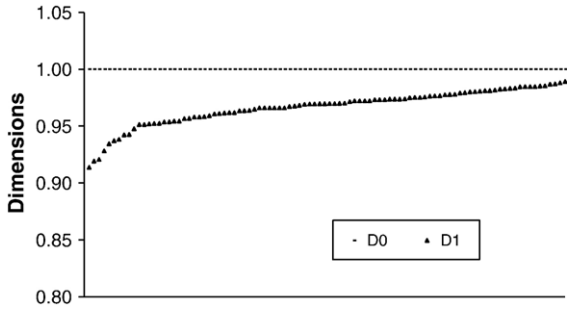

Fig. 5. Capacity dimension, D_0, and entropy dimension, D_1, drawn for increasing values of D_1.

Entropy dimensions, D_1, from particle-size distributions reported by Montero (2005), were in the range 0.77 to 0.88. This study database consisted of 30 samples with contrasting textures, including sandy clay and clay as coarser and finer textural classes. Posadas et al. (2001) analyzed a database with 30 soil samples also, taken from different countries of Europe and America, and with a wide range of clay contents, from 0.3% to 81.2%. The entropy dimensions, D_1, were in the range 0.19 to 1.01. Moreover, 5 out of the 30 particle-size distributions in this data set were Oxisols sampled in Brazil and were characterized by entropy dimensions, D_1, between 0.67 and 0.19, that decreased with increasing clay content.

Oxisols with relatively low D_1 values (Posadas et al., 2001) are soils developed under high intensity weathering conditions over very long periods of time. The underlying saprolite material, which was characterized in this study by D_1 values close to the maximum entropy dimension, had been obviously less affected by weathering. These results are consistent with the interpretation of soils as an open system, resulting from pedogenic processes, which tend to steady state conditions with minimum entropy, much less than in the parent material (Addiscott, 1995; Posadas et al., 2001). In other words, it may be assumed that as the entropy decreases a more ordered system results. In multifractal systems, the dimension, D_1, is a measure of entropy. In this framework, differences in entropy dimensions, D_1, between the Oxisols studied by Posadas et al. (2001) and the saprolite in this work are an expected result. Saprolites behave as a rather disordered system and their particle-size distributions are characterized by a high degree of dispersion, which contrasts with Oxisols that exhibit measures (μ) concentrated in a small region of the particle-size domain. Further studies, including sampling at different depths in the same soil profile, should elucidate the above interpretation of the entropy dimension results.

4.3. Relationship between multifractal parameters and texture

A dependence was found between several parameters derived from the left side ($q>0$) of the $f(\alpha)$ spectra and

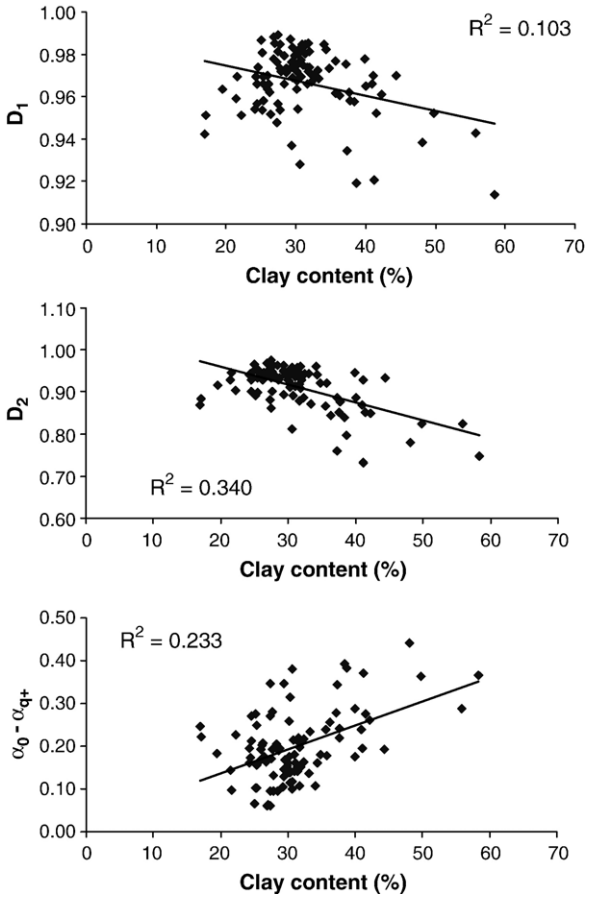

Fig. 6. Capacity dimension, D_0, entropy dimension, D_1, and left-side width, $\alpha_0-\alpha_{max}$, of the $f(\alpha)$ spectra plotted versus clay content.

clay content. Fig. 6 shows that both the entropy dimension, D_1, and the correlation dimension, D_2, exhibited a trend to decrease as the clay content increases. This trend was very weak for the entropy dimension, D_1, but the determination coefficient of linear regression analysis between clay content and the correlation dimension, D_2, was significant ($P<0.05$). Statistically, this means that, as the clay content of the saprolite increases, the entropy dimension tends to decrease and the system is becoming more ordered. The composition of the parent material is not homogeneous and may vary over small distances. As a consequence, even if other pedogenic factors and processes are constant, weathering may result in local patches with different clay contents and different particle-size distributions. This may be the reason for the spatial variability of the soil texture and multifractal parameters derived from measures of particle-size distributions at the study site.

Linear regression analysis also shows a significant ($P<0.05$) positive relationship between clay content and the width of the left side ($\alpha_0-\alpha_{q+}$) of the $f(\alpha)$ spectra (Fig. 6). Moreover, the most positive value of the moment, q_+, used for the evaluation of the $f(\alpha)$ spectra showed a negative correlation ($R^2=0.20$) with clay content. These results indicate that as the clay content increases, i.e. the particle-size distribution is becoming more ordered by the action of pedogenesis, the range of the left side of the $f(\alpha)$ spectra tends to increase and, conversely, the width of the right side tends to decrease. Thus, symmetry features of the $f(\alpha)$ spectra are also related to the clay content and, in the case studied in our work, this dependence may be explained as a result of differential weathering.

The results suggest that parameters of the multifractal spectrum such as the entropy dimension, D_1, the correlation dimension, D_2, and the width or the aperture of the left side ($\alpha_0-\alpha_{q+}$) of the $f(\alpha)$ spectra may be useful as predictive parameters that capture some of the inner details of the particle-size distributions. The relationship between multifractal parameters and clay content is consistent with a high spatial variability of the weathering processes at the study site.

4.4. Statistical analysis of multifractal parameters

Statistical tests (Duncan test) were also conducted to analyze the significance of the mean values of the most important multifractal parameters among the eight randomized treatments in the field revegetation experiment on exposed saprolite. Results of the Duncan test for the eight treatments studied are summarized in Table 3.

The Holder exponent of order zero, α_0, and entropy dimension, D_1, were not significantly different between treatments and depths. Consequently, randomization was able to filter out effects induced by spatial differences in average singularity strength, α_0, and entropy dimension, D_1. These parameters were not relevant in distinguishing the intrinsic variability of the particle-size distributions.

However, other multifractal attributes such as correlation dimension, D_2, the width of the left side ($\alpha_0-\alpha_{q+}$) and the right side ($\alpha_{q-}-\alpha_0$) of the $f(\alpha)$ spectra, and the width of the $f(\alpha)$ spectra itself ($\alpha_{max}-\alpha_{min}$) showed significant differences between treatments (Table 3).

The correlation dimension, D_2, was lowest for treatment 3 and highest for treatment 2. At the 95% confidence level, treatment 3 was significantly different from the other treatments, with the exception of treatments 4 and 5. This result is consistent with the ANOVA analysis of texture, because treatments 3, 4 and 5 exhibit the highest clay contents and the lowest correlation dimension, D_2, values.

Table 3 also shows significant differences between treatments in the width of the $f(\alpha)$ spectra and the ranges

of their left and right sides. The range of the right side ($\alpha_{q-}-\alpha_0$) of the $f(\alpha)$ spectra was highest for treatment 7 and lowest for treatment 2, whereas that of the left side ($\alpha_0-\alpha_{q+}$) was highest for treatment 3 and lowest also for treatment 2. Of course, the width of the $f(\alpha)$ spectra ($\alpha_{max}-\alpha_{min}$) was also lowest for treatment 2, contrasting with the highest value obtained for treatment 7, which was significantly different at the 95% confidence level.

In contrast to the above results and also in contrast with the results of the statistical analysis of the textural fractions, the only multifractal parameter exhibiting significant differences between sampling depths at the 95% confidence level (data not shown) was the width of the left side of the $f(\alpha)$ spectra ($\alpha_0-\alpha_{q+}$).

The width of the right side ($\alpha_{q-}-\alpha_0$) of the $f(\alpha)$ spectra followed by the correlation dimension D_2 exhibited the lowest $F1$ value in ANOVA test (data not shown). Thus, these parameters were the most sensitive for discriminating between randomized treatments. Further investigation is needed to evaluate the consequences of these differences in the structural features of particle-size distributions have on the results of the field trials.

The $f(\alpha)$ spectra indicate that the particle-size distributions may be modeled as multifractal objects. Such analyses are tools, considered to be able to reproduce complexity and to distinguish between different variation patterns. The results also suggest that weathering processes at the scale of this study possibly give rise to patterns that reveal structured, non-random, spatial variability of the soil texture. Fractal attributes, being scale independent, may be relevant for intrinsic variability characterization and for designing sampling strategies.

5. Conclusions

Particle-size distributions from a newly developing soil profile after decapitation of an Oxisol exhibited multifractal behavior. The range of values obtained for the entropy dimension, D_1, was between 0.913 and 0.989 and that for the correlation dimension, D_2, between 0.731 and 0.975. Thus, saprolite behaves as a rather disordered system with particle-size distribution characterized by high dispersion that contrasts with published reports for Oxisols.

A dependence was found between several parameters derived from the left side ($q>0$) of the $f(\alpha)$ spectra and clay content. Both the values of the entropy dimension, D_1, and the correlation dimension, D_2, tend to decrease as the clay content increases. The decrease in the entropy dimension, D_1, is an indication that saprolite is becoming more ordered as the clay content increases, i.e. weathering intensity.

Statistical differences in sand, silt and clay contents among treatments and depths were found, indicating that the texture was far from homogeneous in space over the study area.

The Holder exponent of order zero, α_0, and entropy dimensions, D_1, were not significantly different between treatments and depths. However, several multifractal attributes such as correlation dimension, D_2, the width of the left side ($\alpha_0-\alpha_{q+}$) and the right side ($\alpha_{q-}-\alpha_0$) of the $f(\alpha)$ spectra, and the width of the $f(\alpha)$ spectra itself ($\alpha_{max}-\alpha_{min}$) showed significant differences between treatments.

Acknowledgements

This work was performed in the frame of research project PHB 2003-0043-PC, financed by CAPES (Brazil) and MEC (Spain). The AECI contribution under projects B/0975/03 and B/1035/03 is also acknowledged. Authors are grateful to three anonymous referees for providing valuable comments.

References

Addiscott, T.M., 1995. Entropy and sustainability. Eur. J. Soil Sci. 46, 161–168.

Alves, M.C., 2001. Recuperação de um subsolo utilizado para terraplena e fundaçao da Usina Hidroelétrica de Ilha Solteira, SP. Ilha Solteira, Tese de Livre Docencia. Faculdade de Engenharia. UNESP, Ilha Solteira, São Paulo, Brazil (In Portuguese).

Caniego, J., Martín, M.A., San José, F., 2001. Singularity features of pore-size distribution in soil: singularity strength analysis and entropy spectrum. Fractals 9, 305–316.

Carter, M.R., Gregorich, E.G., Anderson, D.W., Doran, J.W., Janzen, H.H., Pierce, F.J., 1997. Concepts of soil quality and their significance. In: Gregorich, E.G., Carter, M.R. (Eds.), Soil Quality for Crop Production and Ecosystem Health. Elservier Science, Amsterdam, pp. 1–20.

Chhabra, A.B., Jensen, R.V., 1989. Direct determination of the $f(\alpha)$ singularity spectrum. Phys. Rev. Lett. 62, 1327–1330.

Doran, J.W., Parkin, T.B., 1994. Defining and assessing soil quality. In: Doran, J.W., Coleman, D.C., Bezdicek, D.F., Stewart, B.A. (Eds.), Defining Soil Quality for a Sustainable Environment. SSSA Spec. Publ., vol. 35. Soil Sci. Soc. Am., Madison, WI, pp. 3–21.

EMBRAPA, 1999. Sistema Braileiro de Clasificaçao de solos. EMBRAPA Solos, Rio de Janeiro. 412 pp (In Portuguese).

European Environment Agency, 2000. Down to the Earth: Soil Degradation and sustainable Development in Europe. Environmental Issue Series, vol. 16. 31 pp.

FAO, 1998. World Reference Base for Soil Resources. World Soil Resources Report, vol. 60. FAO, Rome, Italy. 88 pp.

Feder, J., 1988. Fractals. Plenum Press, New York.

Gregorich, E.G., 2002. Quality. In: LAL, R. (Ed.), Encyclopedia of Soil Science. Marcel Dekker, Inc., pp. 1058–1061.

Grout, H., Tarquis, A.M., Wiesner, M.R., 1998. Multifractal analysis of particle size distributions in soils. Environ. Sci. Technol. 32, 1176–1182.

Kravchenko, A., Boast, C.W., Bullock, D.G., 1999. Multifractal analysis of soil spatial variability. Agron. J. 91, 1033–1041.

Martín, M.A., Montero, E., 2002. Laser diffraction and multifractal analysis for the characterization of dry soil volume-size distributions. Soil Tillage Res. 64, 113–123.

Martín, M.A., Rey, J.M., 2000. On the role of Shannon's entropy as a measure of heterogeneity. Geoderma 98, 1–3.

Martín, M.A., Taguas, F.J., 1998. Fractal modelling, characterization and simulation of particle size distributions in soil. Proc. R. Soc. Ser. A 454, 1457–1468.

Martín, M.A., Rey, J.M., Taguas, F.J., 2001. An entropy-based parametrization of soil texture via fractal modelling of particle-size distributions. Proc. R. Soc. Lond. Ser. A 457, 937–948.

Martín, M.A., Rey, J.M., Taguas, F.J., 2005. An entropy-based heterogeneity index for mass-size distributions in earth science. Ecol. Model. 182, 221–228.

Meakin, P., 1991. Fractal aggregates in geophysics. Rev. Geophys. 29, 317–354.

Montero, E., 2005. Rényi dimensions analysis of soil particle-size distributions. Ecol. Model. 182, 305–315.

Montero, E., Martín, M.A., 2003. Hölder spectrum of dry grain volume-size distributions in soil. Geoderma 12, 197–204.

Paz Ferreiro, J., 2002. Propiedades de un suelo decapitado en proceso de rehabilitación. MSc Thesis. University of Coruña, Spain (In Spanish).

Paz González, A., Vieira, S.R., Taboada Castro, M.T., 2000. The effect of cultivation on the spatial variability of selected properties of an umbric horizon. Geoderma 97, 273–292.

Posadas, A.N.D., Giménez, D., Bitelli, M., Vaz, C.M.P., Flury, M., 2001. Multifractal characterization of soil particle-size distributions. Soil Sci. Soil Am. J. 65, 1361–1367.

Posadas, A.N.D., Giménez, D., Quiroz, R., Protz, R., 2003. Multifractal characterization of soil pore systems. Soil Sci. Soil Am. J. 67, 1361–1369.

SAS Institute, 1999. SAS user's guide. Version 8. Ed. SAS Inst., Cary, NC.

Soil Survey Staff Division, 1993. Soil Survey Manual. USDA Handb., vol. 18. U.S. Gov. Print. Office, Washington, DC.

Solie, J.B., Raun, W.R., Stone, M.L., 1999. Submeter spatial variability of selected soil and Bermudegrass production variables. Soil Sci. Soc. Am. J. 63, 1724–1733.

Turcotte, D.L., 1986. Fractals and fragmentation. J. Geophys. Res. 91, 1921–1926.

Tyler, S.W., Wheatcraft, S.W., 1992. Fractal scaling of soil particle-size distributions: analysis and limitations. Soil Sci. Soc. Am. J. 56, 362–369.

Vicsek, T., 1992. Fractal Growth Phenomena, 2nd ed. World Scientific Publishing, Singapore.

Vieira, S.R., Hatfield, J.L., Nelsen, D.R., Biggar, J.W., 1983. Geostatistical theory and application to variability of some agronomical properties. Hilgardia 51 (3), 1–75.

Voss, R.F., 1988. Fractals in nature: from characterization to simulation. In: Peitgen, H.O., Saupe, D. (Eds.), The Science of Fractal Images. Springer-Verlag, New York.